Brazilian Journal of Physics
ISSN: 0103-9733
luizno.bjp@gmail.com
Sociedade Brasileira de Física
Brasil

Braz J Phys (2016) 46:157–162
DOI 10.1007/s13538-015-0394-z

GENERAL AND APPLIED PHYSICS

Ion-Acoustic Vortices in Two-Electron-Temperature Magnetoplasma with Cairn's Distributed Electrons and in the Presence of Ion Shear Flow

Q. Haque[1] · Arshad M. Mirza[2] · Javed Iqbal[3]

Received: 16 October 2015 / Published online: 11 January 2016

Abstract Linear and nonlinear characteristics of electrostatic waves in a multicomponent magnetoplasma comprising of Boltzmann distributed electrons, Cairn's distributed hot electrons, and cold dynamic ions are studied. It is found that the effect of superthermal electrons, ion-neutral collisions, and ion shear flow modifies the propagation of ion-acoustic and drift waves. The growth rate of the ion shear flow instability varies with the addition of Cairn's distributed hot electrons. It is also investigated that the behavior of different type of vortices changes with the inclusion of superthermal hot electrons. The relevance of this investigation in space plasmas such as in auroral region and geomagnetic tail is also pointed out.

Keywords Ion-acoustic vortices · Two-electron temperature · Nonthermal distribution of ions

1 Introduction

In different plasma environments such as auroral ionosphere, magneto-tail, Earth's bow shock as well as in the laboratory, two distinct populations of electrons (hot and cold) have been observed ([1] and the references therein). Observations [2] of Earth's magnetosphere have shown the presence of highly energetic electrons with non-Maxwellian distribution. In recent years, a number of researches [3–5] showed their interest in the study of space plasmas by considering the non-Maxwellian behavior of energetic species. The distribution of plasma species having more energetic/superthermal particles in the tail deviates from the Maxwellian distribution. In nonthermal distributions like kappa distribution [6], Cairn's distribution [7] have been proposed by different scientists on the basis of observed space data and theoretical models.

A lot of research work has appeared in the literature, considering the superthermality effect on the propagation of linear and nonlinear waves [8–18]. The role of highly energetic electrons on the formation of acoustic-like solitary waves has been discussed in many references, e.g., Gill et al. [8] investigated the role of superthermal electrons on the propagation of ion-acoustic solitary waves and double layers with the help of reductive perturbation method. Saini et al. [9] used a pseudopotential method to investigate the characteristics of arbitrary amplitude ion-acoustic solitary waves for non-Maxwellian electrons with cold ions. El-Awady et al. [19], investigated the propagation of nonlinear solitary waves in nonextensive electron-positron-ion (e-p-i) plasmas.

Shan and Haque [14] investigated the role of superthermal electrons on the propagation of ion-acoustic and drift wave-driven vortices (which are different structures in nature as compared to solitons, because these structures posses the vorticity). Adnan et al. [15] extended this work to e-p-i plasmas and studied the superthermality effect of electrons and positrons on the characteristics of vortices. The role of superthermal electrons on the linear and nonlinear behavior of ion temperature gradient (ITG mode and ITG-mode driven vortices) has been studied by Batool et al. [16] and Zakir et al. [17], respectively.

✉ Arshad M. Mirza
a_m_mirza@yahoo.com

1 Theoretical Physics Division, PINSTECH, P. O. Nilore, Islamabad, Pakistan

2 Theoretical Plasma Physics Group, Department of Physics, Quaid-i-Azam University, Islamabad 45320, Pakistan

3 Department of Mathematics, Quaid-i-Azam University, Islamabad 45320, Pakistan

Recently, Rufi et al. [20–21] investigated the ion-acoustic solitons and super solitons in a magnetized plasma having two types of electrons. They assumed the Cairn's distribution for the highly energetic electrons and Maxwell-Boltzmann behavior of other inertialess electrons along with dynamic cold ions. They concluded that the inclusion of nonthermal hot electrons extends the Mach number domain to the supersonic regime. In this paper, we considered a model similar to that of Rufi et al. [20], along with ion shear flow along the magnetic field lines, and investigated the role of superthermal electrons (Cairn's distributed hot electrons) on the characteristics of the dipolar and street-type vortices. We also found the modified behavior of the shear flow instability in the presence of highly energetic electrons.

In Section 2, the model equations and the derivation of nonlinear set of equations are presented. The linear dispersion relation is discussed in Section 3. The nonlinear solutions in the form of vortices are discussed in Section 4. The results are summarized in Section 5.

2 Derivation of Nonlinear Equations

Let us consider the propagation of ion-acoustic waves in a three-component highly magnetized and collisional plasma having two types of electrons such as cold electrons following the Boltzmann distribution and the hot electrons following the nonthermal Cairn's type distribution with cold fluid ions. The ambient magnetic field is assumed to be uniform and pointing in the z-direction such that $\mathbf{B}_0 = B_0\hat{\mathbf{z}}$. The electric field can be written as $\mathbf{E} = -\nabla\varphi$, where φ is the electrostatic wave potential. In equilibrium, the three-component plasma satisfies the following quasineutrality condition

$$n_{c0} + n_{h0} = n_{i0}, \tag{1}$$

where the subscript c (h) stands for the cold (hot) species of electrons and i is used for the ions. For nonthermal electron population, the electron distribution function (Cairn's type) [7] can be written as

$$f_{h0}(\upsilon) = \frac{n_{h0}}{(3\alpha+1)\sqrt{2\pi\upsilon_{th}^2}}\left(1+\frac{\alpha\upsilon^4}{\upsilon_{th}^4}\right)\exp\left(-\frac{\upsilon^2}{2\upsilon_{th}^2}\right), \tag{2}$$

where n_{h0} represents the equilibrium density of nonthermal electrons, $\upsilon_{th} = \sqrt{T_h/m_e}$ is the thermal speed of hot electrons, and α is the nonthermal parameter. Here, T_h is the equilibrium temperature of the hot electrons expressed in the energy units. With the nonthermal electron distribution in the presence of ion-acoustic wave potential, we replace $(\upsilon/\upsilon_{th})^2$ by $(\upsilon/\upsilon_{th})^2 - 2e\phi/T_h$ and integrate over velocity space; we obtain the number density of hot electrons,

$$n_h = n_{h0}\left(1-\beta\left(\frac{e\phi}{T_h}\right)+\beta\left(\frac{e\phi}{T_h}\right)^2\right)\exp\left(\frac{e\phi}{T_h}\right), \tag{3}$$

where $\beta = 4\alpha/(1+3\alpha)$. For $\alpha = 0$, it corresponds to Boltzmann distribution of hot electrons. On the other hand, the other group of cold electrons follows the Boltzmann distribution, such that we can write

$$n_c = n_{c0}\exp\left[\frac{e\phi}{T_c}\right], \tag{4}$$

where T_c represents the temperature of cold electrons expressed in the energy units.

To convince, we shall use the following nomenclature: the cold electron density ratio $f = n_{c0}/n_{i0}$, $\alpha_c = T_{\text{eff}}/T_c$, $\alpha_h = T_{\text{eff}}/T_h$, and effective temperature $T_{\text{eff}} = T_c/(f+(1-f)\tau)$ with $\tau = T_c/T_h$. n_{i0} is the total ion number density, and T_i and $T_h(T_c)$ are the fixed temperatures of the ion and hot(cold) electrons expressed in the energy units. We have expanded Eq. (3) $n_h = n_{h0}(1-f)(1-\beta(\alpha_h\Phi)+\beta(\alpha_h\Phi)^2)\exp(\alpha_h\Phi)$. By assuming $\alpha_h\phi \ll 1$, the perturbed part of hot electrons can be written as $n_{h1} \simeq n_{i0}(1-f)(1-\beta)(\alpha_h\Phi_1)$, where the normalized electrostatic potential $\Phi = e\phi/T_{\text{eff}}$. Here, we have used the quasineutrality condition in equilibrium such that $n_{i0} = n_{c0} + n_{h0}$.

The linearized form of Poisson's equation and the usage of Eqs. (3) and (4) yield the following result,

$$\begin{aligned} n_{i1} &\simeq (f\alpha_c + (1-f)(1-\beta)\alpha h)\Phi_1 - \lambda_D^2\nabla^2\Phi_1 \\ &= \delta\Phi_1 - \lambda_D^2\nabla^2\Phi_1 \end{aligned} \tag{5}$$

where $\delta = (f\alpha_c + (1-f)(1-\beta)\alpha_h)$ and $\lambda_D = \sqrt{T_{\text{eff}}/4\pi n_{i0}e^2}$. The subscripts zero (0) and one (1) denote the equilibrium and the perturbed quantities, respectively. n_{c1}, n_{h1} are the perturbed number densities of cold and hot electrons, respectively.

The momentum equation for the cold, collisional ions can be written as

$$m_i n_{i0}(\partial_t + \mathbf{v}_i\cdot\nabla)\mathbf{v}_i = en_{i0}\left(-\nabla\phi + \frac{1}{c}\mathbf{v}_i\times\mathbf{B}_0\right) - m_i n_{i0}\nu_{in}\mathbf{v}_i \tag{6}$$

Here, we have neglected the pressure gradient of the cold ions by assuming that the phase velocity of the wave is much larger than the thermal speed of ions and ν_{in} is the collision frequency between the ions and neutral particles. However, we have ignored the self-collisions as well as the electron-ion and electron-neutral collisions, because of the small inertia of the electrons.

For low-frequency waves ($\partial_t \ll \omega_{ci}$, where $\omega_{ci} = eB_0/m_i c$ is the ion gyrofrequency), the perpendicular component of cold ion fluid Eq. (6) with the help of drift approximation can be written as

$$\mathbf{v}_{i\perp} \simeq \frac{c}{B_0}\hat{z}\times\nabla\phi - \frac{c}{B_0\omega_{ci}}(\partial_t + v_{in} + \mathbf{v}_E\cdot\nabla + (v_{i0}(x) + v_{iz})\partial_z)\nabla_\perp\phi. \quad (7)$$

Similarly, the parallel component of ion fluid in the presence of parallel ion shear flow can be written as

$$\begin{aligned}(\partial_t + v_{in} + \mathbf{v}_E\cdot\nabla + (v_{i0}(x) + v_{iz})\partial_z)v_{iz} \\ = -\frac{e}{m_i}\partial_z\phi + \mathbf{v}_E\cdot\nabla v_{i0}(x) \\ = -\frac{T_{\text{eff}}}{m_i}\left(\partial_z - \frac{\partial_x v_{i0}(x)}{\omega_{ci}}\partial_y\right)\left(\frac{e\phi}{T_{\text{eff}}}\right) \\ = -c_s^2(\partial_z - S_i\partial_y)\Phi\end{aligned} \quad (8)$$

where $S_i = \partial_x v_{i0}/\omega_{ci}$ is the parallel velocity ion shear flow parameter and $c_s = \sqrt{T_{\text{eff}}/m_i}$ is the effective ion-acoustic speed.

Using ion continuity equation and drift approximation (7), we get

$$\begin{aligned}(d_t + v_{in} + \mathbf{v}_E\cdot\nabla + v_{iz}\partial_z)\frac{n_{i1}}{n_{i0}} - \frac{c}{B_0\omega_{ci}}(d_t + v_{in} + \mathbf{v}_E\cdot\nabla + v_{iz}\partial_z)\nabla_\perp^2\phi \\ -v_{in}\frac{n_{i1}}{n_{i0}} - \frac{c\partial_x(\ln n_{i0})}{B_0}\partial_y\phi + \partial_z v_{iz} = 0,\end{aligned} \quad (9)$$

where $d_t = \partial_t + v_{i0}(x)\partial_z$ and $\mathbf{v}_E = (c/B_0)\hat{z}\times\nabla\varphi$ is the usual $\mathbf{E}\times\mathbf{B}_0$ drift. Here, we have used the condition $|\mathbf{v}_E\cdot\nabla| \gg |v_z\partial_z|$. It is worth to mention here that $\nabla\times\mathbf{v}\neq 0$ can give rise to a vortex-type structure in the nonlinear regime. Equations (5), (8), and (9) form a closed set of equations.

3 Linear Dispersion Relation

To obtain a linear dispersion relation, we linearize our set of nonlinear Eqs. (5), (8), and (9) and assume that all the perturbed quantities are proportional to $\exp[-i(\omega t - k_y y - k_z z)]$ and finally obtain the following dispersion relation,

$$(\omega' + iv_{in})^2 k_\perp^2\rho_i^2 + \delta(\omega' + iv_{in})\left(\omega'\left(1 + \frac{k^2\lambda_D^2}{\delta}\right) - \omega_*\right) - k_z^2 c_s^2\left(1 - \frac{k_y S_i}{k_z}\right) = 0, \quad (10)$$

where $\omega' = \omega - k_z v_{i0}(x)$ is the Doppler shifted frequency, $\rho_i = c_s/\omega_{ci}$ is the effective ion Larmor radius, $\omega_* = (k_y c T_{\text{eff}}\partial_x \ln n_{i0})/(\delta e B_0)$ is the modified drift wave frequency, and $S_i = \partial_x v_{i0}(x)/\omega_{ci}$ is the almost constant ion shear flow parameter.

In the absence of collisions and background density gradients with $k^2\lambda_D^2 \ll 1$, Eq. (10) reduces to

$$\omega' = k_z c_s\sqrt{\frac{1 - k_y S_i/k_z}{f\alpha_c + (1-f)(1 - 4\alpha/(1+3\alpha))\alpha_h + k_\perp^2\rho_i^2}}, \quad (11)$$

which shows that the ion-acoustic mode can become unstable for $k_y S_i > k_z$. Figure 1 shows a plot of normalized growth rate γ/ω_{ci} vs. $k_z\rho_i$ by choosing the same parameters as described in [21], i.e., $n_{i0} = 0.1/\text{cm}^3$, $B_0 = 0.2$ G, $T_h = 500$ eV, $T_c = 5$ eV, $f = 0.1$, $\tau = 0.04$, $M = u/c_s = 0.98$, $k_y = \sqrt{0.5}/\rho_s$, $S_i = 0.5$, by varying the nonthermal electron population parameter $\alpha = 0.9$ (black solid curve) and 0.1 (dashed red curve). It is evident from the graph in Fig. 1 that the growth rate of acoustic mode in the presence of shear increases with the increase of nonthermal electron population.

On the other hand, if we keep the ion drag, Eq. (10) predicts an oscillatory instability of the ion-acoustic drift waves in the presence of hot nonthermal and cold electrons for $\omega' \ll v_{in}$. Letting $\omega = \omega_r + i\gamma$, we get

$$\gamma = -\frac{v_{in}k_\perp^2\rho_s^2}{\delta} - \frac{k_z^2 c_s^2(1 - k_y S_i/k_z)}{v_{in}\delta}. \quad (12)$$

Equation (12) shows that in the absence of parallel ion shear flow, the wave is purely damped, however, the ion drift dissipative instability gives growth for $|S_i|k_y > k_z$. Therefore, it follows from Eq. (12) that ion-acoustic and drift waves can be driven unstable by the combined effects of ion shear flow provided the condition $|S_i|k_y > k_z$ is met. The ion shear flow and ion-neutral collisions can drive the coupled ion-acoustic and drift modes unstable for two electron species plasmas.

4 Nonlinear Analysis

In the nonlinear case, to find a localized vortex-type solution, we first use the following normalization for mathematical as well as numerical simplicity: the time variable with inverse of ion cyclotron frequency ω_{ci}^{-1}, the space coordinates with the effective ion Larmor radius $\rho_i = c_s/\omega_{ci}$, the ion fluid velocity with effective ion-acoustic speed $c_s = \sqrt{T_{\text{eff}}/m_i}$, and the

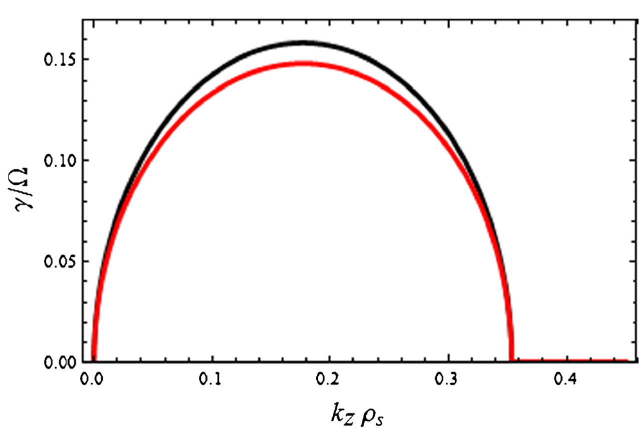

Fig. 1 (Colored online): The growth rate is plotted as a function of k_z from Eq. (11) by choosing some typical parameters given in the text. The *top black curve* for $\alpha = 0.9$ and *below the red curve* for $\alpha = 0.1$

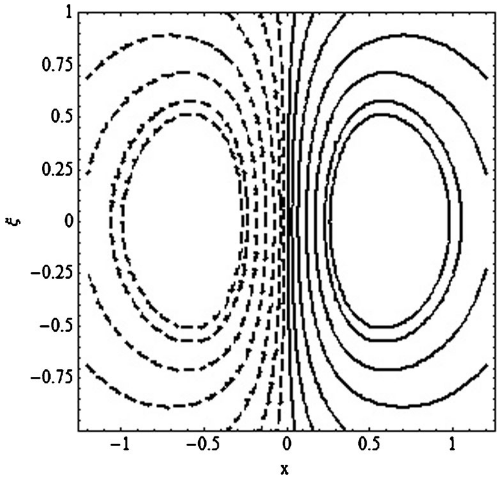

Fig. 2 (Colored online): The typical contour plots for the normalized electrostatic potential ϕ in (x, ξ) plane from Eqs. (26) and (27) are drawn by choosing some typical parameters given in the text. The said *curves* correspond to a Mach number $M = u/c_s = 0.98, S_i = 0.1$. Here, all the distances are normalized with ρ_i

perturbed ion number density with its total equilibrium number density. In the normalized form, the ion continuity and momentum equations for collisionless plasma can be expressed as follows:

$$\partial_t n_i + \nabla\cdot(n_i \mathbf{v}_i) = 0, \tag{13}$$

$$(\partial_t + \mathbf{v}_i\cdot\nabla)\mathbf{v}_i = -\nabla\Phi + \mathbf{v}_i \times \hat{z}, \tag{14}$$

Using drift approximation in the ion continuity equation and letting $n_i = n_{i0} + n_{i1}$, (where $n_{i1} \ll n_{i0}$, and n_{i0}, n_{i1} are the equilibrium and perturbed number densities of ions, respectively), we obtain

$$D_t\left(n_{i1} - \nabla_\perp^2 \Phi\right) - (\partial_x \mathrm{In}\, n_{i0})\partial_y \Phi + \partial_z v_{iz} = 0,$$

where $D_t = d_t + \hat{z}\times\nabla\perp\Phi\cdot\nabla + v_{iz}\partial_z$. Using (5), the above equation can be rewritten as

$$D_t\left(\delta\Phi - \left(1| + \lambda_D^2/\rho_i^2\right)\nabla_\perp^2\Phi\right) - (\partial_x \mathrm{In}\, n_{i0})\partial_x\Phi + \partial_z v_{iz} = 0. \tag{15}$$

Here, we have assumed $\nabla_\perp^2 \gg \partial^2/\partial z^2$.

The parallel component of ion momentum equation is

$$D_t v_{iz} = -\partial_z\Phi + S_i\partial_y\Phi, \tag{16}$$

Next, we shall proceed to obtain the possible stationary solution [22] of Eqs. (15) and (16). We introduce a new frame (x, ξ), such that $\xi = y + \eta z - ut$, where u is the translational speed of the vortex and η is the angle between the wave front normal and xy-plane. It may be noted here that we have assumed that $|\hat{z}\times\nabla\perp\Phi\cdot\nabla| \gg |v_{iz}\partial_z|$. Equation (15) in the transformed frame can be written as

$$-U\mathscr{L}_\phi v_{iz} = -(\eta - S_i)\partial_\xi\Phi, \tag{17}$$

where $\mathscr{L}_\phi = \partial_\xi - (1/U)(\partial_x\Phi\partial_\xi - \partial_\xi\Phi\partial_x)$ is a differential operator and $U = u - \eta v_{i0} \neq 0$. It can be easily verified that in the stationary frame Eq. (17) is exactly satisfied by

$$v_{iz} = \frac{1}{U}(\eta - S_{i0})\Phi. \tag{18}$$

Inserting v_{iz} from Eq. (18) into Eq. (15), we get

$$U\mathscr{L}_\phi\left(\delta\phi - \left(1 + \lambda_D^2/\rho_i^2\right)\nabla_\perp^2\Phi\right) - (\partial_x \mathrm{In}\, n_{i0})\partial_\xi\Phi + \frac{\eta}{U}(\eta - S_{i0})\partial_\xi\Phi = 0,$$

which on simplification gives

$$\left(\delta - \frac{U_{n*}}{U} - \frac{\eta(\eta - S_{i0})}{U^2}\right)\partial_\xi\Phi + \left(1 + \frac{\lambda_D^2}{\rho_i^2}\right)\left[\partial_\xi - \frac{1}{U}\hat{z}\times\nabla\perp\Phi\cdot\nabla\right]\nabla_\perp^2\Phi = 0, \tag{19}$$

where $U_{n*} = \partial_x \mathrm{In}\, n_{i0}$. For $\left(\delta - \frac{U_{n*}}{U} - \frac{\eta(\eta - S_{i0})}{U^2}\right) = 0$, we obtain the following equation

$$\partial_\xi\nabla_\perp^2\phi - \frac{1}{U}J\left[\phi, \nabla_\perp^2\phi\right] = 0, \tag{20}$$

where $\nabla_\perp^2 = \partial_x^2 + \partial_\xi^2$. The above equation is satisfied by

$$\nabla_\perp^2\Phi = \frac{4\Phi_0}{R^2}\exp\left[-\frac{2}{\phi_0}(\Phi - U_x)\right] \tag{21}$$

where Φ_0 and R_0 are arbitrary constants. The analytical solution of Eq. (21) is

$$\Phi = Ux + \Phi_0 \mathrm{In}\left[2\cosh x + 2\left(1 - \frac{1}{R_0^2}\right)\cos\xi\right]. \tag{22}$$

For $R_0^2 > 1$, the vortex profile given in Eq. (22) resembles the Kelvin-Stuart "cats eyes" that are chains of vortices [23]. The vortex chain speed is $U = \left[U_{n*} \pm \sqrt{(U_{n*})^2 + 4\eta(\eta - S_{i0})}\right]/2$. Although an exact solution of the nonlinear equations can only be obtained with the help of numerical simulations, which are beyond the scope of our present investigation. Here, we shall present some interesting analytical solutions which highlight the importance of new results. On the other hand, if we retain the Jacobian nonlinearity, we have

$$\partial_\xi\nabla_\perp^2\Phi - \frac{1}{U}J\left[\Phi, \nabla_\perp^2\Phi\right] - \psi_1\partial_\xi\Phi = 0, \tag{23}$$

where $\psi_1 = \left(-\delta + \frac{U_{n*}}{U} + \frac{\eta(\eta - S_{i0})}{U^2}\right)\left(1 + \frac{\lambda_D^2}{\rho_i^2}\right)^{-1}$. The solution of Eq. (23) can be written as

$$\nabla_\perp^2\Phi - \psi_1\Phi = f(\Phi - Ux) \tag{24}$$

The function $f(\Phi - Ux) = F*(\Phi - Ux)$ is assumed to behave linearly, where F is some constant. Thus, Eq. (24) gives us

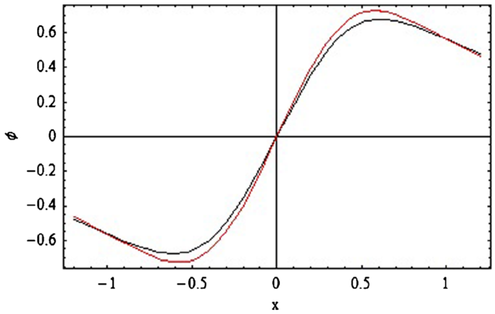

Fig. 3 (Colored online): The two-dimensional view of dipolar vortex obtained from Eqs. (26) and (27) for the same parameters as described in the text and for $\alpha = 0.9$ and $\alpha = 0.1$ cases with fixed Mach number $M = 0.98$, where $\alpha = 0.1$ (*red curve*) and $\alpha = 0.9$ (*black curve*)

$$\nabla_\perp^2 \Phi - \psi_1 \Phi = F^*(\Phi - Ux). \tag{25}$$

Equation (25) can be transformed in (r, θ) coordinates, and its solution in the outer ($r < R_0$) and inner ($r > R_0$) regions of a circle of arbitrary radius R_0 can be written as

$$\phi_{out}(r,\theta) = C_1 K_1(\psi_1 r)\cos\theta \tag{26}$$

and

$$\Phi_{in}(r,\theta) = \left[C_2 J_1(\psi_2 r) + \left(\frac{\psi_1^2 + \psi_2^2}{\psi_2^2}\right) U r\right]\cos\theta, \tag{27}$$

respectively, where $\psi_2^2 = -(\psi_1^2 + F), F = -(\psi_1^2 + \psi_2^2)$ and K_1, J_1 are modified and ordinary Bessel functions, respectively. The arbitrary constants C_1 and C_2 can be evaluated from the continuity of the solution $\Phi, \partial_r \Phi$, and $\nabla_\perp^2 \Phi$ at the boundary of the circle $r = a_0$ as

$$C_1 = U\frac{a_0}{K_1(\psi_1 a_0)}, \; C_2 = U\left(-\frac{\psi_1^2}{\psi_2^2}\right)\frac{a_0}{J_1(\psi_2 a_0)}, \tag{28}$$

and ψ_2 from the following nonlinear solution

$$\frac{K_2(\psi_1 a_0)}{K_1(\psi_1 a_0)} = -\frac{\psi_1 J_2(\psi_2 a_0)}{\psi_2 J_1(\psi_2 a_0)}. \tag{29}$$

The above Eqs. (26) and (27) along with arbitrary constants admit the dipolar vortex solution. The contour plot of the solutions (26) and (27) is plotted in Fig. 2 for the same parameters as discussed earlier. We find $\rho_i = 6196.3$ cm. It can be seen that like the vortex street solutions, the nonlinear dipolar structures are also formed on a short scale length, i.e., of the order of Larmor radius $_i$. Equation (26) implies that the dipolar solution will be bounded if $\psi_1 > 0$, that is $\left(-\delta + \frac{U_{n^*}}{U} + \frac{\eta(\eta - S_{i0})}{U^2}\right) > 0$. Thus, the boundedness condition of the dipolar solution modifies in the presence of Cairn's factor (α) which is contained in δ. Similarly, the range of Mach number will also change with the superthermal effects of electrons.

5 Summary

In this paper, linear as well as nonlinear propagation of electrostatic waves has been investigated in the presence of Cairn's distributed hot electrons and ion shear flow parallel to the ambient magnetic field. The linear dispersion relation is derived, and the instability condition ($|S_i|k_y > k_z$) due to shear flow is also discussed. The growth rate of the instability is plotted for the space plasma parameters, and its variation with the superthermal electrons is shown. It is noticed that the growth rate increases with the superthermality factor of electrons. On the other hand, various types of coherent nonlinear vortex solutions (such as monopolar, dipolar, and vortex street) are found in a collisionless plasma limit. It is observed that the inclusion of the superthermality effect modifies the condition of existence and boundedness of vortex solutions (see e.g., Fig. 3). The results of the present investigation may be beneficial to understand the dynamics of two temperature electrons of space plasmas.

Acknowledgments This research work was partially supported by the Quaid-i-Azam University Research Fund (URF) Project (2015–2016).

References

1. B. Bezzerides, D.W. Forslund, E.L. Lindman, Phys. Fluids **21**, 2179 (1978)
2. S.P. Christon, D.G. Mitchell, D.J. Williams, L.A. Frank, C.Y. Huang, E. EastmanT, J. Geophys. Res. **93**, 2562 (1988)
3. P. Schippers, M. Blanc, N. André, I. Dandouras, G.R. Lewis, L.K. Gilbert, A.M. Persoon, N. Krupp, D.A. Gurnett, A.J. Coates, S.M. Krimigis, D.T. Young, M.K. Dougherty, J. Geophys. Res. **113**, A07208 (2008)
4. S. Baboolal, R. Bharuthram, M.A. Hellberg, J. Plasma Phys. **41**, 34 (1989)
5. T.K. Baluku, M.A. Hellberg, R.L. Mace, J. Geophys. Res. **116**, A04227 (2011)
6. M. Vasyliunas, J. Geophys. Res. **73**, 2839 (1968)
7. R.A. Cairns, A.A. Mamun, R. Bingham, R. Bostrom, R.O. Dendy, C.M.C. Nairn, P.K. Shukla, Geophys. Res. Lett. **22**, 2709 (1995)
8. T.S. Gill, P. Bala, H. Kaur, N.S. Saini, S. Bansal, J. Kaur, Eur. Phys. J. D **31**, 91 (2004)
9. N.S. Saini, I. Kourakis, M.A. Hellberg, Phys. Plasmas **16**, 062903 (2009)
10. B. Sahu, Phys. Plasmas **17**, 122305 (2010)
11. M.N. Kadijani, H. Abbasi, H.H. Pajouh, Plasma Phys. Control. Fusion **53**, 025004 (2011)
12. C.R. Choi, K.W. Min, T.N. Rhee, Phys. Plasmas **18**, 092901 (2011)
13. B. Basu, Phys. Plasmas **15**, 042108 (2008)
14. S.A. Shan, Q. Haque, Phys. Plasmas **19**, 084503 (2012)
15. M. Adnan, S. Mahmood, A. Qamar, Phys. Plasmas **21**, 092119 (2014)
16. N. Batool, W. Masood, A.M. Mirza, Phys. Plasmas **19**, 082111 (2012)

17. U. Zakir, Q. Haque, A. Qamar, A.M. Mirza, Astrophys. Space Sci. **350**, 565 (2014)
18. H. Abbasi, H.H. Pajouh, Phys. Plasmas **14**, 012307 (2007)
19. E.I.E.I. Awady, S.A.E.I. Tantaway, W.M. Moslem, P.K. Shukla, Phys. Lett. A **374**, 3216 (2010)
20. O.R. Rufai, R. Bharuthram, S.V. Singh, G.S. Lakhina, Phys. Plasmas **21**, 082304 (2014)
21. O.R. Rufi, R. Bharuthram, S.V. Singh, G.S. Lakhina, Commun Nonlinear Sci. Numer Simulat **19**, 1338 (2014)
22. V.D. Larichev, G.M. Resnik, Dokl. Akad. Nauk SSSR **231**, 1077 (1976)
23. L. Stenflo, Phys. Fluids **30**, 3297 (1987)